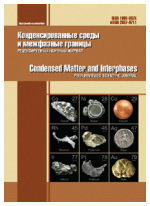

ISSN 1606-867X (Print)
ISSN 2687-0711 (Online)
Condensed Matter and Interphases
Kondensirovannye Sredy i Mezhfaznye Granitsy
https://journals.vsu.ru/kcmf/

**Original articles**

Research article
https://doi.org/10.17308/kcmf.2023.25/10977

# Hydrogen permeability of the Pd–Pb system foil of various composition

**N. B. Morozova[1]✉, A. I. Dontsov[1.2], A. I. Fedoseeva[1], A. V. Vvedenskii[1]**

[1]*Voronezh State University,*
*1 Universitetskaya pl., Voronezh 394018, Russian Federation*

[2]*Voronezh State Technical University,*
*84 ul. 20-Letiya Oktyabrya, Voronezh 394006, Russian Federation*

**Abstract**

The purpose of the study was identification of the role of the chemical composition of Pd, Pb-alloys based of palladium in the processes of injection and extraction of atomic hydrogen.

The objects of study were Pd-Pb alloy foils with a lead content of 3, 5, 7, 9, and 11 at. %, representing the β-phase of the solid solution. Samples with a thickness of 40 to 62 μm were obtained by cold rolling. Hydrogen permeability was studied by cyclic voltammetry and two-stage cathode-anode chronoamperometry in deaerated solutions of 0.1 M $H_2SO_4$. The obtained results were processed according to a mathematical model developed for electrodes of semi-infinite thickness.

The dependence of the hydrogen permeability coefficient, as well as the rate constants of the processes of injection and extraction of atomic hydrogen, on the chemical composition of the alloy has been revealed. It was found that the Pd–Pb alloy with a lead content of 5 at.% demonstrates the highest values of hydrogen permeability compared with samples of the same crystal structure, since the rate constant of atomic hydrogen injection is very sensitive to the alloy structure. The latter confirms that the phase-limiting transition of atomic hydrogen into the alloy is the rate-determining stage, at least in the initial period of time.

**Keywords:** Solid solution of Pd-Pb systems, Atomic hydrogen, Phase boundary transition, Alloy structure, Hydrogen permeability, Cathode injection, Anode extraction

***Funding:*** The work was supported by the Ministry of Science and Higher Education of the Russian Federation within the framework of state order to higher education institutions in the sphere of scientific research for 2022-2024, project No. FZGU-2022-0003.

***Funding:*** The study received financial support from the Ministry of Science and Higher Education of the Russian Federation within the framework of State Contract with universities regarding scientific research in 2022–2024, project No. FZGU-2022-0003.

***For citation:*** Morozova N. B., Dontsov A. I., Fedoseeva A. I., Vvedenskii A. V. Hydrogen permeability of the Pd–Pb system foil of various composition. *Condensed Matter and Interphases*. 2023;25(1): 85–94. https://doi.org/10.17308/kcmf.2023.25/10977

Для цитирования: Морозова Н. Б., Донцов А. И., Федосеева А. И., Введенский А. В. Водородопроницаемость фольги системы Pd–Pb разного состава. *Конденсированные среды и межфазные границы*. 2023;25(1): 85–94. https://doi.org/10.17308/kcmf.2023.25/10977

✉ Morozova Natalya Borisovna, e-mail: mnb@chem.vsu.ru


## 1. Introduction

Now, one of the promising areas is the development of materials for portable electronic sensors based on palladium alloys and their oxides [1–3]. Methods for the synthesis of such materials are not expensive and are compatible with planar technologies of the microelectronic industry [4, 5].

An analysis of literature sources indicates that metal oxide semiconductors based on palladium alloys have a significant advantage in detecting gases with oxidizing properties (ozone, nitrogen dioxide) compared to materials with *n*-type of conductivity, in particular tin (IV) oxide $SnO_2$, which is widely used for the detection of reducing gases [6]. However, the process of interaction of palladium alloys and metal oxide semiconductors based on them with reducing gases remains not fully understood.

Also, one of the important areas of hydrogen energetics is the production of high-purity hydrogen using membranes based on palladium and its alloys. Hydrogen is widely used as fuel for ecological transport and in power plants, as well as in industries such as micro- and nanoelectronics and reduction metallurgy [7–9]. Effective palladium membranes should have not only high specific hydrogen permeability and corrosion resistance, but also high plasticity [10, 11]. The forecasting of hydrogen permeability is an important step in the design of fused membranes for hydrogen separation. Hydrogen permeability in alloys is determined by the diffusion coefficient of hydrogen and its solubility. Since in modern technologies the consumption of high-purity hydrogen is in great demand, reduction of the cost of its production becomes necessary. Therefore, the transition from pure metals to alloys is one of the effective ways for reducing the cost of membranes. In addition, doping palladium with such chemical elements as Pb, Ru, Cu, Y, and Ag can increase the durability of the membrane [12–15].

The Pd-Pb system exhibits limited solubility over the entire range of compositions and temperatures. The investigated samples of alloys of the Pd-Pb system with a lead content of up to 14 at. % are substitutional solid solutions [16]. It was also shown in [17] that the Pd–Pb system has a fairly wide range of α-solubility compared to other binary palladium compounds. An analysis of the research results [12] showed that the addition of lead to palladium-based alloys leads not only to an increase in their hydrogen permeability, but also to an increase in corrosion resistance, strength, and plasticity. The fact that binary Pb–Pd alloys have an excellent ability to accumulate atomic hydrogen is also important [18].

The aim of this research was investigation of the role of the chemical composition of palladium-based Pd,Pb alloys in the processes of injection and extraction of atomic hydrogen.

## 2. Experimental

The studies were carried out on foils made of palladium-lead solid solution with a Pb content 3, 5, 7, 9, and 11 at. % obtained by cold rolling. The foil thickness of the Pd-Pb system ranged from 40 to 62 μm.

The studied samples were made in an electric arc furnace in a purified helium environment at a slight overpressure [12]. Pd–Pb systems were fused with lead and palladium with a purity of 99.95 wt. %. Each ingot was subjected to remelting 2–3 times, which allowed ensuring the uniformity of the composition. Then, the flat samples were melted from the original ingots for subsequent rolling into foil. The chemical composition of the alloy was controlled by scanning electron microscopy (SEM, Jeol-6510, Japan). The structure and phase composition of Pd,Pb samples were studied by X-ray diffractometry (ARL X'TRA, Switzerland).

For obtaining foil of a given thickness, the annealed samples were subjected to cold rolling followed by vacuum annealing at 950°C for 3 h, and then rolling on a four-high rolling mill in 10 passes with intermediate vacuum annealing at 900 °C for 30–90 min. The use of this technology allows to obtain foils with a uniform fine-grained structure of a solid solution with an FCC lattice. The electrode made of spectrally pure graphite, onto which metal samples, previously degreased with ethyl alcohol were deposited using a conductive graphite glue, was used for electrochemical measurements.

The studies were carried out in a glass three-electrode cell with the cathode and anode spaces separated by a thin section. The working solution was aqueous 0.1 M $H_2SO_4$ (extra pure

grade), prepared using a bidistillate. Solutions were deaerated with chemically pure argon for 30 min. Platinated platinum Pt(Pt) was used as an auxiliary electrode. Copper sulphate reference electrode (0.1M $CuSO_4$ +0.1M $H_2SO_4$) was connected to the working electrode with a Luggin capillary and a thin section.

Electrochemical measurements were performed by cyclic voltammetry and two-stage cathode-anode chronoamperometry using an IPC-Compact potentiostat. Before obtaining the polarization dependences, the working electrode was subjected to preliminary preparation, for the removal of the products of oil annealing used in rolling, as well as for standardization of the surface condition. The preparation included preliminary polarization of the electrode for 500 s at the initial potential $E_{pp}$ = 0.21 V, followed by cycling over a wide range of potentials. First, the potential was scanned from $E_p$ to the cathode region $E_c$ = -0.13 V, then the scanning direction was changed to the anode region up to $E_a$ = 1.55 V and again returned to $E_{pp}$. The potential scan rate was 5 mV/s. According to this scheme, the samples were cycled four times without preparation of the electrode surface and changing the solution. Potentiodynamic curves (forward and reverse) were obtained in the same range of potentials at d$E$/d$t$ = 5 mV/s.

The potential $E_{pp}$ = 0.21 V was applied to the working electrode for 500 s before obtaining each two-stage cathode-anode $i$,$t$-curve. The curve corresponding to the cathode current transients was recorded at the hydrogenation potential $E_c$ = −0.13 V, the hydrogenation potential values were the same for all studied samples. The duration of the hydrogenation process $t_c$ of electrodes was changed from 1 to 10 s. Then the potential was switched to the hydrogen ionization potential $E_p^a$ determined based on the anodic peak in the cyclic voltammogram. The current transients was recorded until it reached a constant value, which usually occurred within 500 s. After that, without turning off the cell and without removing the electrode from the cell, the pre-polarization potential $E_{pp}$ was again applied and the procedure with another time $t_c$ was repeated. The hydrogenation time used in the study $t_c$ = 10 s removed the possibility of palladium hydrides being formed.

All potentials are provided for a standard hydrogen electrode, and the current values are given per single unit of the visible surface.

## 3. Results and discussion

Hydrogen permeability depends on many factors, such as the roughness, structure, substructure, and phase composition of metal systems. Diffraction patterns of the studied Pd,Pb alloys with different lead content are shown in Fig. 1. The orientation of the (200) and (220) faces was most pronounced in alloys with a lead content of 3, 5, 9, and 11 at. %. This orientation is characteristic of cold-rolled samples due to grain elongation during rolling. The texture (111) and (311) was characteristic for an alloy with a lead content of 7 at. %. As can be seen from Fig. 1, the orientation of the faces of Pd-7 at. % Pb alloy was close to the orientation for pure palladium obtained under the same conditions.

The values of the crystal lattice parameters for alloys of the Pd–Pb system, obtained at different pretreatment temperatures in a vacuum are shown in Table 1 [12].

As can be seen from the data in the Table, an increase in the lead content in the alloy of the Pd–Pb system from 3 to 11 at. % results in a nonlinear change in the period of the crystal lattice, which reached a minimum at $X_{Pb}$ = 5 at. %.

The production of thin metal alloys by cold rolling involves the use of organic oils. Subsequent annealing of rolled samples at temperatures of 900 and 950 °C results in the formation of annealing products on the surface of the alloys. The presence of such products manifested itself on the anodic branches of the potentiodynamic curves as a suppression of the ionization peak of atomic hydrogen and

**Table 1.** Lattice parameter of Pd–Pb alloys during vacuum heat treatment [12]

| $t$, °C | $X_{Pb}$, at.% | | | | |
|---|---|---|---|---|---|
| | 3 | 5 | 7 | 9 | 11 |
| 25 | 3.9080±0.0005 | 3.9027±0.0007 | 3.9286±0.0007 | 3.9422±0.0003 | 3.9480±0.0002 |
| 200 | 3.9168±0.0005 | 3.9114±0.0013 | 3.9369±0.0002 | 3.9511±0.0010 | 3.9567±0.0006 |

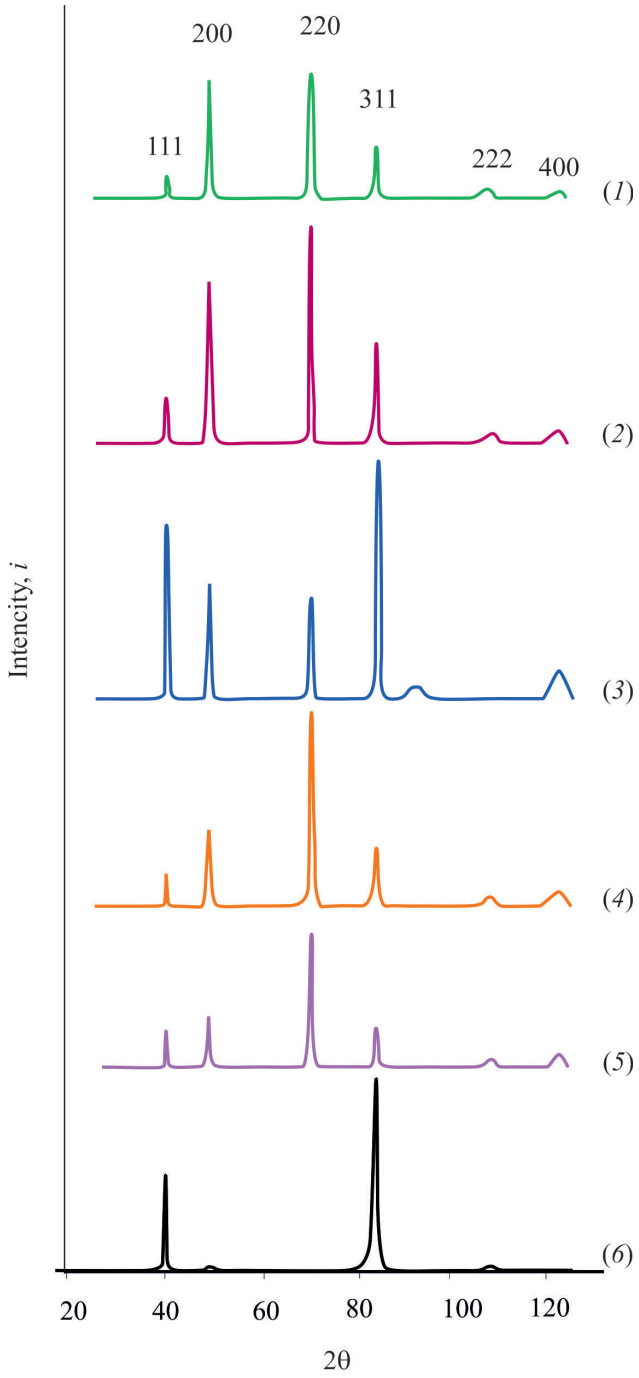


**Fig. 1.** X-ray diffractograms of Pd-Pb alloys foil with lead content: 3(*1*), 5 (*2*), 7 (*3*), 9 (*4*), 11 at. % (*5*) and Pd (*6*)

the appearance of a peak in the potential range from 1.00 to 1.20 V (Fig. 2). This peak, which was clearly visible both in the first and second cycles of voltammograms, was probably associated with the oxidation of oil annealing products on the surface of the rolled foil. Further cycling of the potential significantly increased the height of the

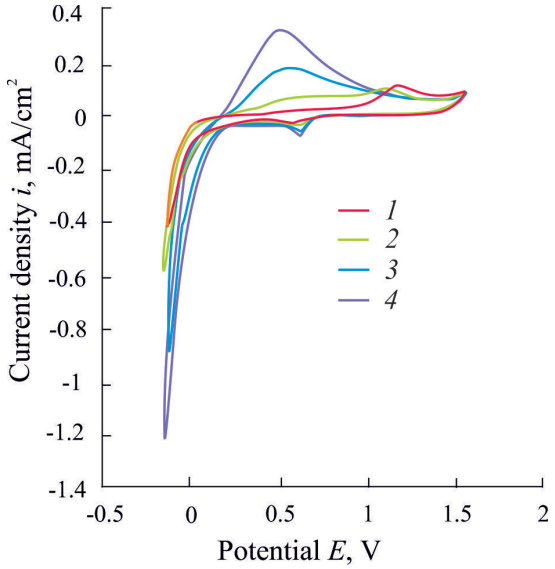


**Fig. 2.** Cyclic voltammograms for Pd-7 alloy foil at.% Pb obtained in 0.1 M $H_2SO_4$ at *dE/dt* = 5 mV/s; *1-4* – cycle numbers

atomic hydrogen ionization peak, and results in the disappearance of the oxidation peak. Five or more scan cycles did not lead to any noticeable changes in the obtained results.

Thus, the cyclic voltammetry method not only turned out to be sensitive to contamination of the surface of metal samples, but also allowed additional surface cleaning to be performed.

Cyclic voltammograms obtained on the foil electrodes of the Pd–Pb system with different lead content are shown in Fig. 3. The comparison of cyclic voltammograms revealed that 3 at.% of lead in the alloy results in a sharp increase in the ionization peak of atomic hydrogen compared to pure palladium. However, an increase in the concentration of lead to 11 at. % results in a decrease in the ionization rate of atomic hydrogen. The cathodic branch of the curve at a potential of ~0.65 V had a peak related to the reduction of surface palladium oxides, presumably PdO. The position and amplitude of this peak were practically independent of the lead concentration in the alloy. The observed maximum cathode current corresponds to the process of evolution of molecular hydrogen.

For the calculation of the hydrogen permeability parameters two-stage cathode-anode chronoamperograms of samples of the Pd-Pb system were used (Fig. 4). Their general view was similar for all alloys, however, as

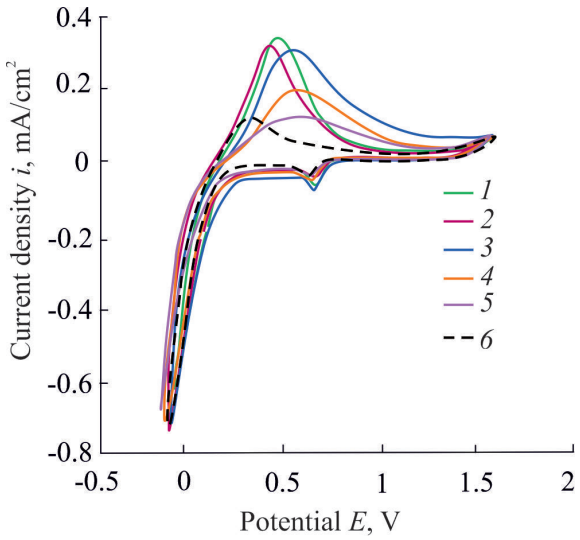


**Fig. 3.** Cyclic voltammograms for foil alloys of the Pd-Pb system with $X_{Pb}$ = 3 (1), 5 (2), 7 (3), 9 (4), 11 (5) at. % and palladium (6) obtained in 0.1 M $H_2SO_4$ at $dE/dt$ = 5 mV/s

the hydrogenation time increased, a gradual increase in anodic and cathodic currents was observed. It should be noted that if the nature of the declines on the anode and cathode *i,t*-curves for alloys with $X_{Pb}$ up to 7 at. % was quite sharp, for alloys with a lead content of 9 and 11 at. %, the currents decrease more smoothly, which may be due to a change in the mechanism of the process.

As in the case of rather slow cyclic voltammograms, the pulsed cathodic and anodic current transients with an increase in lead content up to $X_{Pb}$ = 7 at. % first increased and then decreased. Therefore, the addition of Pb to the palladium crystal lattice in an amount of more than 7 at. % results in the suppression of both the intercalation process and the ionization of atomic hydrogen.

Using the results presented in [19], and taking into account the thickness of the studied samples, further processing of the experimental data was carried out using a mathematical model describing the injection and extraction of atomic hydrogen for electrodes of semi-infinite thickness [20]. This model assumes that during the period of hydrogenation $t_c$ = 10 s, there is no through penetration of atomic hydrogen into the foil. In this case, according to [20], for the studied samples, the cathode current transients $i_c$ is described by the equation:

$$i_c(t) = i_c^{\infty} + F\overleftarrow{k}\left(c_{\bar{H}}^{s}(\eta_c) - c_{\bar{H}}^{e}\right)\cdot\exp\left(\frac{\overleftarrow{k}^2 t}{D_H}\right)\mathrm{erfc}\frac{\overleftarrow{k}t^{1/2}}{D_H^{1/2}}. \quad (1)$$

Here $i_c^{\infty}$ is the maximum cathodic current, $D_H$ is the diffusion coefficient of atomic hydrogen in the solid phase, $\vec{k}$ is the efficient rate constant of atomic hydrogen extraction, $\Delta c_{\bar{H}} = (c_{\bar{H}}^{s}(\eta^c) - c_{\bar{H}}^{e})$ is the change in the concentration of atomic hydrogen $\bar{H}$ in the surface layer of the metal phase $c_{\bar{H}}^{e}$, and $c_{\bar{H}}^{s}$ is the equilibrium molar concentration $\bar{H}$ in the bulk and in the near-

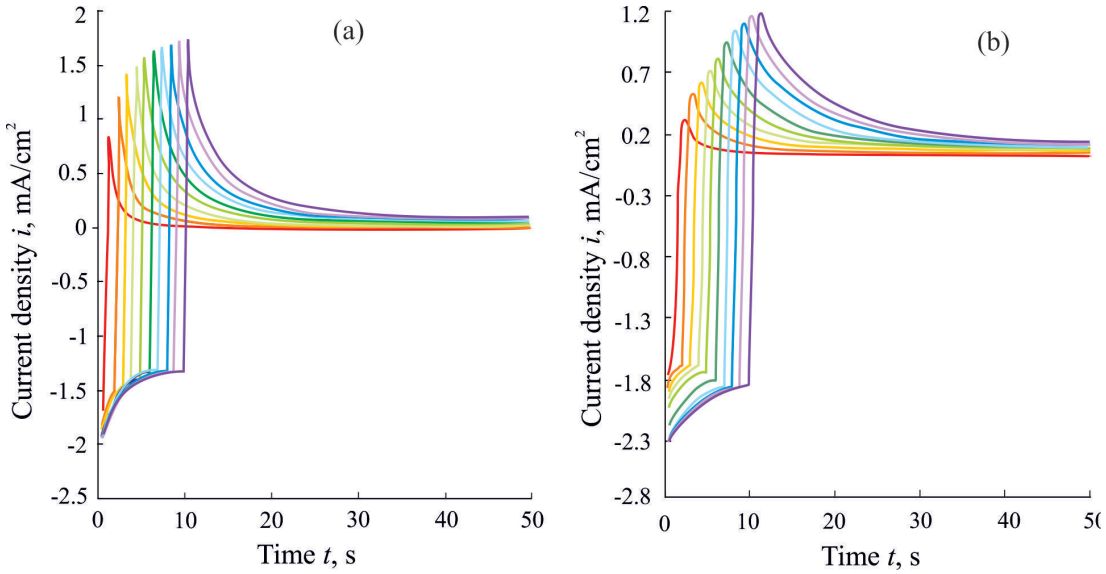


**Рис. 4.** Двухступенчатые катодно-анодные хроноамперограммы, полученные в 0.1 M $H_2SO_4$ для фольги системы Pd–Pb с содержанием свинца 5 (а) и 11 ат. % (б)

surface layer of the film, respectively, and $\eta_c$ is the cathodic overvoltage.

For short times when $t \leqslant 3$ s, and the parameter $\frac{\overleftarrow{k}t^{1/2}}{D_H^{1/2}} \ll 1$, equation (1) describes the initial period of the cathodic current transients, when the phase boundary kinetics mode is reached:

$$i_c(t) = i_c(0) - F\overleftarrow{k}\left[c_{\bar{H}}^{s}(\eta_c) - c_{\bar{H}}^{e}\right]\frac{2\overleftarrow{k}t^{1/2}}{\pi^{1/2}D_H^{1/2}}. \quad (2)$$

In case when $\frac{\overleftarrow{k}t^{1/2}}{D_H^{1/2}} \gg 1$, which means that the limiting stage is the solid-phase diffusion H, equation (1) is transformed:

$$i_c(t) = i_c^{\infty} + \frac{FK_D}{\pi^{1/2}t^{1/2}}. \quad (3)$$

Here $K_D = \Delta c_{\bar{H}} \cdot D_H^{1/2}$ is the coefficient that makes it possible to estimate the permeability of hydrogen into the metal in the case when the values $\Delta c_{\bar{H}}$ and $D_H$ cannot be determined separately.

The linearisation of cathodic chronoamperograms obtained at $t_c$ = 10 s, allowed to isolate two linear segments (Fig. 5). Their location, both at short and longer times, strongly depends on the concentration of palladium in the alloy. At the same time, the slopes of the obtained dependences not significantly differed from each other. This suggests that with an increase in the concentration of lead in the Pd,Pb-alloy, the mechanism of hydrogen insertion/ionization does not change.

Diffusion and kinetic parameters obtained from the linear dependences of the cathodic current transients are presented in Table 2:

Analysing the obtained parameters, we can conclude that the hydrogen permeability parameter $K_D$ grows with an increase in the concentration of lead in the palladium crystal lattice, reaching a maximum value in the alloy with $X_{Pb}$ = 7 at. %. A further increase in the lead content in the alloy results in a non-systematic change in the parameters.

The comparison of similar characteristics on Pd-Pb samples with pure palladium revealed that even small additions of lead to the palladium crystal lattice results in the suppression of the processes of incorporation and ionization of atomic hydrogen in the alloy. At the same time, the calculated values of the parameters determined for the alloy with $X_{Pb}$ = 7 at. %, almost coincide with the values corresponding to palladium.

It should be noted that the effective rate constant of the extraction $\vec{k}$ for all the studied alloys remain practically unchanged within the experimental error. At the same time, the effective rate constant of the process of injection of atomic hydrogen $\overleftarrow{k}$ varied with the change in lead content in the alloy. As in the case of hydrogen permeability, these characteristics were maximal for an alloy containing 7 at. % Pd. As a consequence, the adsorption equilibrium constant $K$ changed in the same way.

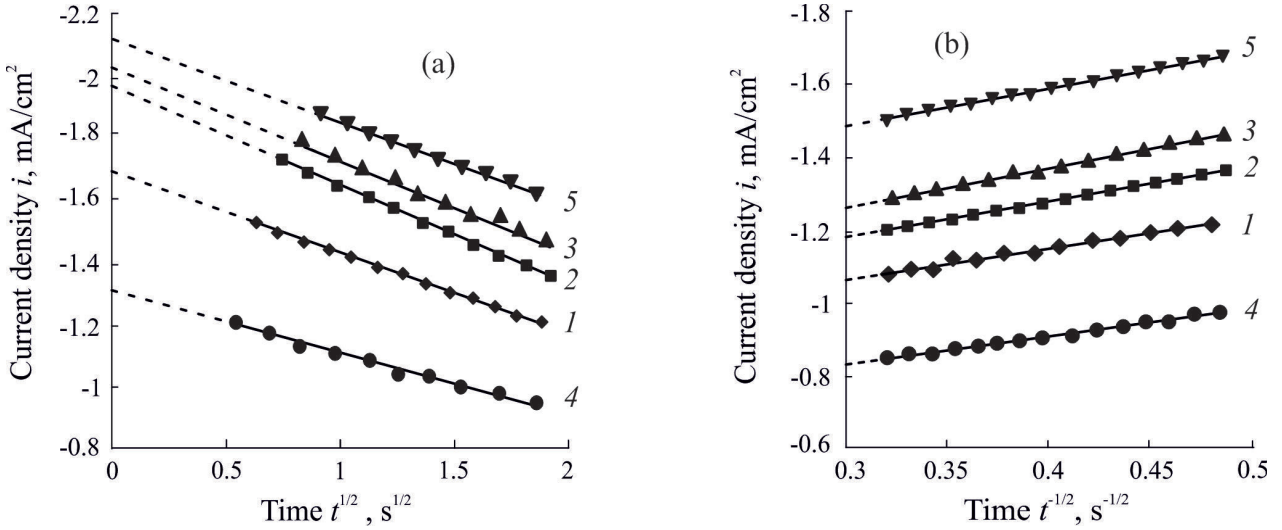


**Fig. 5.** Linearised cathodic potentiostatic current transients curves for Pd-Pb alloy samples with $X_{Pb}$ = 3 (*1*), 5 (*2*), 7 (*3*), 9 (*4*), eleven (*5*) at. % for different time sections: a) $t$ = 0-3 s; b) $t$ = 4-10 s

**Table 2.** Characteristics of cathode injection and anode extraction of atomic hydrogen obtained both on the foil of the Pd-Pb system with different lead content and on Pd [21]

| $X_{Pb}$, at. % | $K_D \cdot 10^8$, mol/cm$^2$·s$^{1/2}$ | $\vec{k} \times 10^8$, mol/cm$^2$·s | $\overleftarrow{k} \times 10^4$, cm/s | $K \cdot \times 10^5$, mol/cm$^3$ |
|---|---|---|---|---|
| 0 | 2.06 ± 0.76 | 1.88 ± 0.47 | 2.43 ± 0.86 | 5.57 ± 2.24 |
| 3 | 1.07 ± 0,01 | 1.12 ± 0.04 | 3.77 ± 0.05 | 3.32 ± 0.02 |
| 5 | 1.40 ± 0.01 | 1.35 ± 0.01 | 3.07 ± 0.05 | 4.36 ± 0.01 |
| 7 | 2.02 ± 0.01 | 1.79 ± 0.01 | 3.24 ± 0.13 | 5.63 ± 0.01 |
| 9 | 0.65 ± 0.01 | 0.58 ± 0.05 | 3.21 ± 0.02 | 1.84 ± 0.01 |
| 11 | 1.64 ± 0.01 | 1.66 ± 0.01 | 3.05 ± 0.02 | 5.08 ± 0.01 |

The values $\overleftarrow{k}$ and $\vec{k}$ determined in these experiments are important characteristics of the phase-boundary exchange process. The most favourable orientation of a metal sample for surface processes is the (311) crystal face, which manifests itself in an alloy with $X_{Pb}$ = 7 at. %. However, based on the obtained results, we can conclude that the results on hydrogen permeability for an alloy with 7 at. % cannot be compared with data for alloys of other compositions due to the different structure of the alloy. On the other hand, there was a non-monotonic decrease in both the diffusion and kinetic parameters of hydrogen permeability for alloys with $X_{Pb}$ >7 at. %. In this regard, it should be noted that the alloy used in the study with $X_{Pb}$ = 11 at. % had additional deformations associated with the folds of the sample. The latter could lead to an increase in the hydrogen permeability parameter.

The theoretical model developed for samples of semi-infinite thickness adequately describes the processes of cathodic injection and anodic extraction of atomic hydrogen on the studied alloys of the Pd–Pb system with different lead content. In particular, the complete anode current transients of step chronoamperograms is adequately described by the equation:

$$i_a(\tau) = i_a^{\infty} - \frac{F[c_{\text{H}}^{s}(\eta_c) - c_{\text{H}}^{c}]}{\pi^{1/2} t^{1/2}} D_{\text{H}}^{1/2} \times \left(1 - \frac{\overleftarrow{k}\pi^{1/2} t^{1/2}}{D^{1/2}}\right) \exp\frac{\overleftarrow{k}^2 \tau}{D_{\text{H}}} \operatorname{erfc}\frac{\overleftarrow{k}\tau}{D_{\text{H}}^{1/2}}. \quad (4)$$

Here $\tau = t - t_c$. In the anodic chronoamperogram (4), it is not possible to identify the sections corresponding to the phase boundary transition and diffusion processes separately. Therefore, the processes of injection and extraction of atomic hydrogen were considered only within the framework of the solid-phase diffusion kinetics regime. We assumed that, at sufficient times, these processes are limited only by solid-phase diffusion of atomic hydrogen in a metal sample. Taking into account this assumption, the section of the anode *i,t*-curve at $t$ > 50 s was well linearised in the coordinates $i_a - [1/\tau^{1/2} - 1/t^{1/2}]$ according to the equation:

$$i_a(\tau) = i_a^{\infty} - \frac{FK_D}{\pi^{1/2}}\left(\frac{1}{\tau^{1/2}} - \frac{1}{t^{1/2}}\right). \quad (5)$$

The value of the hydrogen permeability coefficient $K_D$ can also be found from the slope of the chronocoulograms plotted in coordinates $q_a(\tau) - [\tau^{1/2} + t_c^{1/2} - t^{1/2}]$ according to the equation:

$$q_a(\tau) \approx i_a^{\infty}\tau + \frac{2FK_D}{\pi^{1/2}}\left[\tau^{1/2} + t_c^{1/2} - t^{1/2}\right]. \quad (6)$$

The parameters of the injection and extraction processes of atomic hydrogen, determined using the linear dependences of the anode current transients, are presented in Table 3.

One can see from these data, the hydrogen permeability coefficient calculated based on the anode current transients was somewhat overestimated compared to $K_D$ calculated based on cathode current transients (Fig. 6). Possibly,

**Table 3.** Hydrogen permeability coefficients calculated from anodic chronoamperograms and chronocoulograms for Pd-Pb system foils with different lead content

| $X_{Pb}$, at.% | 3 | 5 | 7 | 9 | 11 |
|---|---|---|---|---|---|
| $K_D$ ($i_a$)×10$^8$, mol/cm$^2$·s$^{1/2}$ | 3.01 ± 0.04 | 4.41 ± 0.01 | 14.27 ± 0.30 | 1.49 ± 0.02 | 8.08 ± 0.30 |
| $K_D$ ($q_a$)×10$^8$, mol/cm$^2$·s$^{1/2}$ | 4.86 ± 0.02 | 4.54 ± 0.02 | 7.11 ± 0.15 | 16.33 ± 0.05 | 23.87 ± 0.09 |

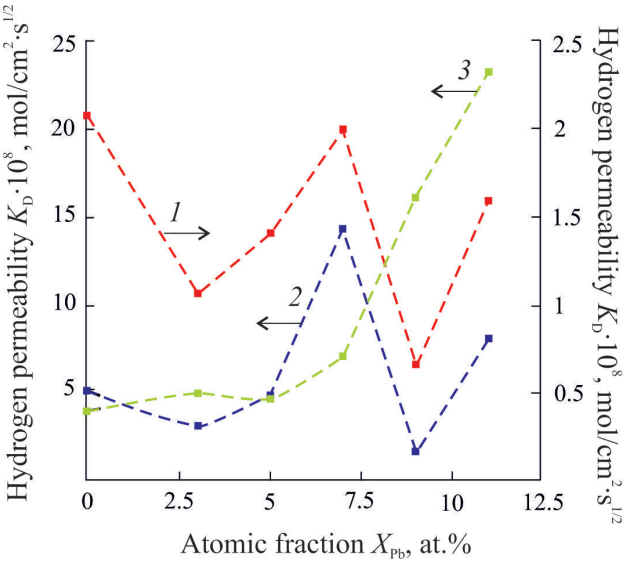


**Fig. 6.** Dependence of $K_D$ on the composition of the alloy, found from the cathode (*1*) and anodic chronoamperograms (*2*) and chronocoulograms (*3*)

this phenomenon is due to the effect of dilatation of the crystal lattice of palladium-based alloys. It should be noted that the nature of the $K_D$ dependencies determined based on the cathode and anode chronoamperograms (Fig. 6) on the composition of the alloy was almost the same. At the same time, the $K_D$ values, calculated based on chronocoulograms, non-linearly increase with an increase in the lead content in the alloy. The reasons for this discrepancy are not yet clear.

Lead additives strengthen palladium. Out of the studied alloys, a sample with a lead content of 11 at. % had higher hardness (HV) and higher tensile strength ($\sigma_B$) than the other samples [12]. As a result, this sample was more prone to the formation of macrodefects, which adversely affect the hydrogen permeability. In addition, this composition is close to peritectic for the Pd–Pb system, which can also affect the electrochemical behaviour of the sample.

Based on the presented X-ray patterns (Fig. 1), we can conclude that the alloy containing 7 at. % Pb is very similar to pure palladium by crystallographic orientation. Therefore, a comparison of the hydrogen permeability of alloys with a Pb content of 7 and 11 at. % with alloys of other compositions is incorrect. Therefore, among Pd,Pb alloys with a lead content of 3, 5, and 9 at.%, the alloy with $X_{Pb}$ = 5 at.% was characterized by the highest hydrogen permeability. In this case, alloys of the same crystallographic orientation were considered.

The data obtained are consistent with the results presented in [12]. However, the indicated values of hydrogen permeability, obtained using the physical method of the calibrated volume, did not reveal a noticeable effect based on the orientation of the crystal face. At the same time, the electrochemical method of non-stationary chronoamperometry used in this study turned out to be sufficiently sensitive to the structural state of the sample surface.

## 4. Conclusions

1. The injection and extraction of atomic hydrogen of the studied Pd-Pb samples of different compositions, obtained by cold rolling, is adequately described by a mathematical model developed for electrodes of semi-infinite thickness.

2. Potentiodynamic and chronoamperometric dependences for alloys of the Pd-Pb system with lead content $X_{Pb} \leqslant 11$ at. % showed that small additions of lead to palladium did not change the kinetics of hydrogen evolution. An alloy with a lead content of 5 at. % demonstrated the best hydrogen permeability among the alloys of the Pb–Pd system, considering samples with the same structure.

3. It was established that when lead is added in an amount of up to 7 at. % into the crystal lattice of palladium, both the atomic hydrogen ionization rate and hydrogen permeability increased. However, a further increase in the lead content in the alloy results in suppression of the process. At the same time, the addition of lead results in a decrease in the hydrogen permeability constant $K_D$, as well as the effective rate constant of atomic hydrogen injection $\vec{k}$ compared to pure palladium.

4. The electrochemical method of chronoamperometry turned out to be quite sensitive to the structural state of the sample surface. The alloy structure especially affected the phase-boundary exchange stage, which was reflected in the effective rate constant of atomic hydrogen injection.

### Contribution of the authors

The authors contributed equally to this article.

## Conflict of interests

The authors declare that they have no known competing financial interests or personal relationships that could have influenced the work reported in this paper.

## References

1. Marikutsa A. V., Rumyantseva M. N., Gaskov A. M., Samoylov A. M. Nanocrystalline tin dioxide: Basics in relation with gas sensing phenomena. Part I. Physical and chemical properties and sensor signal formation, *Inorganic Materials*, 2015;51(13): 1329–1347. https://doi.org/10.1134/s002016851513004x

2. Ryabtsev S. V., Shaposhnik A. V., Samoylov A. M., Sinelnikov A. A., Soldatenko S. A., Kuschev S. B., Ievlev V. M. Thin films of palladium oxide for gas sensors. *Doklady Physical Chemistry*. 2016;470(2): 158–161. https://doi.org/10.1134/S0012501616100055

3. Ievlev V. M., Ryabtsev S. V., Shaposhnik A. V., Samoylov A. M., Kuschev S. B., Sinelnikov A. A. Ultrathin films of palladium oxide for oxidizing gases detecting, *Procedia Engineering*, 2016;168: 1106 –1109. https://doi.org/10.1016/j.proeng.2016.11.357

4. Marikutsa A. V., Rumyantseva M. N., Gaskov A. M., Samoylov A. M. Nanocrystalline tin dioxide: Basics in relation with gas sensing phenomena part II. Active centers and sensor behavior. *Inorganic Materials*. 2016;52(13): 1311–1338. https://doi.org/10.1134/S0020168516130045

5. Ryabtsev S. V., Ievlev V. M., Samoylov A. M., Kuschev S. B., Soldatenko S. A., Microstructure and electrical properties of palladium oxide thin films for oxidizing gases detection. *Thin Solid Films*. 2017;636: 751–759. https://doi.org/10.1016/j.tsf.2017.04.009

6. Korotcenkov G., Cho B. K. Ozone measuring: What can limit application of $SnO_2$-based conductometric gas sensors? *Sensors and Actuators B*. 2012;161(1): 28–44. https://doi.org/10.1016/j.snb.2011.12.003

7. Slovetsky D. I., Chistov E. M., Roshan N. R. Production of pure hydrogen. *Mezhdunarodnyj nauchnyj zhurnal al'ternativnaja jenergetika i jekologija*. 2004;1(9): 43–46. (In Russ., abstract in Eng). Available at: https://www.elibrary.ru/item.asp?id=9336911

8. Yan F., Xu L., Wang Y. Application of hydrogen enriched natural gas in spark ignition IC engines: from fundamental fuel properties to engine performances and emissions *Journal of Renewable and Sustainable Energy Reviews*. 2018;82(1): 1457–1488. https://doi.org/10.1016/j.rser.2017.05.227

9. Cappelletti A., Martelli F. Investigation of a pure hydrogen fueled gas turbine burner. *International Journal of Hydrogen Energy*. 2017;42(15): 10513–10523. https://doi.org/10.1016/j.ijhydene.2017.02.104

10. Adhikari S., Fernando S. Hydrogen membrane separation techniques. *Industrial & Engineering Chemistry Research*. 2006;45(3): 875-881. https://doi.org/10.1021/ie050644l

11. Paglieri S. N., Way J. D. Innovations in palladium membrane research. *Separation and Purification Methods*. 2002;31(1): 1–169. https://doi.org/10.1081/SPM-120006115

12. Gorbunov S. V., Penkina T. N., Roshan N. R., Chustov E. M., Burkhanov G. S., Kannykin S. V. Palladium–lead alloys for the purification of hydrogen-containing gas mixtures and the separation of hydrogen from them. *Russian Metallurgy (Metally)*. 2017;(1): 54–59. https://doi.org/10.1134/S0036029517010050

13. Ievlev V. M., Roshan N. R., Belonogov E. K., Kushev S. B., Kannikin S. V., Maksimenko A. A., Dontsov A. I., Glazunova Y. I. Hydrogen permeability of foil of Pd-Cu, Pd-Ru and Pd-In-Ru alloys received by magnetron sputtering *Condensed Matter and Interphases*. 2012;14(4): 422-427. (In Russ., abstract in Eng.). Available at: https://www.elibrary.ru/item.asp?id=18485336

14. Iwaoka H., Ide T., Arita M., Horita Z. Mechanical property and hydrogen permeability of ultrafine-grained Pd–Ag alloy processed by high-pressure torsion. *International Journal of Hydrogen Energy*. 2017;42(38): 24176–24182. https://doi.org/10.1016/j.ijhydene.2017.07.235

15. Sakamoto Y., Chen F. L., Kinari Y. Permeability and diffusivity of hydrogen through Pd-Y-In(Sn, Pb) alloy membranes. *Journal of Alloys and Compounds*. 1994;205(1–2): 205–210. https://doi.org/10.1016/0925-8388(94)90790-0

16. Vassiliev V., Mathon M., Gambino M., Bros J. P. The Pd-Pb system: excess functions of formation and liquidus line in the range $0<X_{Pd}>0.60$ and $600<T<1200$ K. *Journal of Alloys and Compounds*. 1994;215(1-2): 141–149. https://doi.org/10.1016/0925-8388(94)90831-1

17. Durusell Ph., Feschotte P. The binary system Pd-Pb. *Journal of Alloys and Compounds*. 1996;236(1-2) 195–202. https://doi.org/10.1016/0925-8388(95)02056-X

18. Gierlotka W., Dębski A., Terlicka S., Saternus M., Fornalczyk A., Gąsior W. On the Pb-Pd system. Calorimetric studies and ab-initio aided thermodynamic calculations. *Journal of molecular liquid*. 2020;316: 113806. https://doi.org/10.1016/j.molliq.2020.113806

19. Fedoseeva A. I., Morozova N. B., Dontsov A. I., Kozaderova O. A., Vvedenskii A. V. Cold-rolled binary palladium alloys with copper and ruthenium: injection and extraction of atomic hydrogen. *Russian Journal of Electrochemistry*. 2022;58(9): 812–822. https://doi.org/10.1134/S1023193522090051

20. Morozova N. B., Vvedenskii A. V., Beredina I. P. The phase-boundary exchange and the non-steady-state diffusion of atomic hydrogen in Cu–Pd and

Ag–Pd alloys. I. Aanalysis of the model. *Protection of metals and physical chemistry of surfaces*. 2014;50(6): 699–704. https://doi.org/10.1134/S2070205114060136

21. Morozova N. B., Vvedensky A. V., Beredina I. P. The phase-boundary exchange and the non-steady-state diffusion of atomic hydrogen in Cu-Pd and Ag-Pd alloys. II. Experimental data. *Protection of metals and physical chemistry of surfaces*. 2015; 51(1): 72–80. https://doi.org/10.1134/S2070205115010098

## Information about of authors

*Natalia B. Morozova*, Cand. Sci. (Chem.), Associate Professor at the Department of Physical Chemistry, Voronezh State University (Voronezh, Russian Federation).

https://orcid.org/0000-0003-4011-6510
mnb@chem.vsu.ru

*Alexey I. Dontsov,* Cand. Sci. (Phys.–Math.), Associate Professor at the Department of Materials Science and Industry of Nanosystems, Voronezh State University; Associate Professor at the Department of Physics, Voronezh State Technical University, Voronezh, Russian Federation; Senior Researcher.

https://orcid.org/0000-0002-3645-1626
dontalex@mail.ru

*Anastasia I. Fedoseeva,* 4th year post-graduate student at the Department of Physical Chemistry, Voronezh State University (Voronezh, Russian Federation).

https://orcid.org/0000-0002-6041-7460
Kanamepsp@yandex.ru

*Alexander V. Vvedenskii,* Dr. Sci. (Chem.), Professor, Professor at the Department of Physical Chemistry, Voronezh State University (Voronezh, Russian Federation).

https://orcid.org/0000-0003-2210-5543
alvved@chem.vsu.ru

*Received 29.11.2022; approved after reviewing 07.12.2022; accepted for publication 15.12.2022; published online 25.03.2023.*

*Translated by Valentina Mittova*
*Edited and proofread by Simon Cox*